Research article

MRC

Received: 21 June 2016 Revised: 13 September 2016 Accepted: 15 September 2016 Published online in Wiley Online Library: 9 October 2016

(wileyonlinelibrary.com) DOI 10.1002/mrc.4528

Stereodynamics of some pyridoxine derivatives

I. Z. Rakhmatullin, L. F. Galiullina, A. A. Balandina, M. R. Garipov, A. D. Strelnik, A. S. Galiullina, Y. G. Shtyrlin and V. V. Klochkov*

ABSTRACT The conformational properties of three pyridoxine derivatives were studied by ^{1}H dynamic NMR spectroscopy. Conformational exchange caused by a rotation of 2-nytrophenyl group around one single C–C bond, of 2,4-dinitrophenyl substituent around two single C–O bonds, and twist-twist transformations of the seven-membered ketal cycle was observed by NMR experiments at low temperatures. Meanwhile, the conformational exchange of the acetal ring remains fast in the NMR timescale even at 198 K. The energy barriers for all observed conformational exchange processes were determined by the lineshape analysis of dynamic NMR spectra. The activation barriers of the 2-nitrophenyl group rotation were almost the same for all studied compounds, about 40–41 kJ/mol. The energy barriers of the conformational exchange processes of the 2,4-nitrophenyl group and the ketal cycle increased significantly up to 10 kJ/mol in comparison with previously studied compounds with similar structure.

Keywords: pyridoxine; energy barrier; dynamic ^{1}H NMR; 2D NOESY NMR; conformational exchange

Introduction

Synthesis of molecular systems with desirable biochemical or physical properties often requires knowledge about spatial structure of compounds and information about their conformational mobility.[1–3] Nowadays, NMR techniques are proved to be a powerful tool for conformational analysis.[4]

In the last decades, acetals and ketals of pyridoxine have been widely used in the synthesis of molecules with important biological and physical activities.[5–9] These compounds contain various substituents at the *ortho* position to the seven-membered acetal cycle. Both of them – the substituent and the cycle – participate in rapid conformational processes, creating a complicated stereochemical picture. The knowledge of the dynamics of these processes and their mutual influence may provide an important tool for studying mechanisms of action for such compounds and designing the structures with an improved activity.

In our previous works, we have studied the pyridoxine derivatives with substituents at the aromatic oxygen atom. It was shown that these compounds are involved into two conformational exchange processes in solution. One is a transformation of seven-membered cyclic fragment between the chair and the twist forms. Another is a rotation of 2,4-dinitrophenyl fragment of the molecules around a rather flexible connection to the pyridine ring by two single bonds.[10–12] Correlations between the steric structure and reactivity of such compounds were also revealed.[13]

In this paper, we present the results of dynamic NMR study of three new pyridoxine derivatives, a potent nonlinear optical materials[14]: 3-isopropyl-8-methyl-6-(2-nitrophenyl)-1,5-dihydro-[1,3]dioxepino[5,6-c]pyridine-9-ol (**I**), 3,3,8-trimethyl-6-(2-nitrophenyl)-1,5-dihydro-[1,3]dioxepino[5,6-c]pyridine-9-ol (**II**), and 9-(2,4-dinitrophenoxy)-3,3,8-trimethyl-6-(2-nitrophenyl)-1,5-dihydro-[1,3]dioxepino[5,6-c]pyridine (**III**) (Fig. 1).

All three compounds contain a seven-membered acetal ring with a 2-nitrophenyl *ortho*-substituent at the six-position of pyridine. In this article, the rotating group is connected to the pyridine ring by one single C–C bond that makes it less flexible, and we expected the stronger influence of the substituent on the conformational process in the seven-member cycle in comparison with previously studied molecules. Compound **III** in addition includes 2,4-dinitrophenyloxy *ortho*-substituent at the opposite side of the acetal ring (Fig. 1). Such molecular configuration creates an interesting conformational picture of two rotors at both sides of the seven-membered cycle and provides a good opportunity to the DNMR study of the influence of rotating groups on the transformations of the acetal ring.

Experimental Section

Materials and NMR data acquisition

Compounds (**I**, **II**, **III**) were synthesized according to the following scheme (Fig. 2).

Compounds **I** and **II** were obtained by addition of 1-bromo-2-nitrobenzene to the DMF solution of the pyridoxine acetal in the presence of 2.5 eq. of potassium *tert*-butylate. Compound **III** was synthesized by the procedure described in the patent[15] using pyridoxine derivative **II** as a starting material.

All of the NMR experiments were performed on a Bruker Avance II 500 NMR spectrometer equipped with a 5-mm probe using standard Bruker TOPSPIN software. The ^{1}H NMR data were collected with 32-k complex data points and were apodized with a Gaussian window function (lb = −0.5 and gb = 0.2) prior to Fourier transformation. ^{1}H NMR spectra were recorded using 90° pulses, a delay between pulses of 2 s, a spectrum width of 10 ppm, and a minimum of ten scans. Signal-to-noise enhancement was achieved by

* *Correspondence to: Vladimir V. Klochkov, Kazan (Volga Region) Federal University, 18 Kremlevskaya St., Kazan 420008, Russia. E-mail: vladimir.klochkov@kpfu.ru*

Kazan (Volga Region) Federal University, 18 Kremlevskaya St., Kazan 420008, Russia

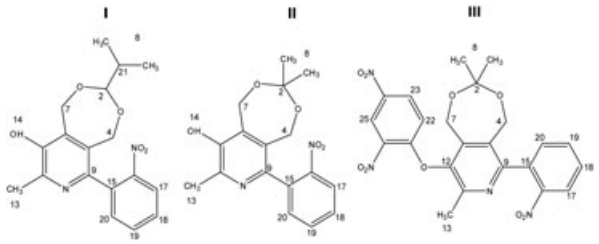

Figure 1. Chemical structures of studied compounds.

multiplication of the free induction decay with an exponential window function (lb = 3 Hz). The accuracy of the chemical shifts and scalar coupling was at least 0.01 ppm.

Assignment of the ^{1}H NMR signals for the entire set of compounds was achieved from the signal multiplicities, the integral values, and the characteristic chemical shifts from the through-bond correlations in the 2D correlation spectroscopy (COSY) spectra, from the through-space correlations in the 2D nuclear Overhauser effect spectroscopy (NOESY) spectra, and from the ^{1}H-^{13}C heteronuclear correlations in the 2D heteronuclear single-quantum correlation (HSQC) and heteronuclear multiple bond correlation (HMBC) spectra.

All 2D experiments were performed with 2 k × 512 data points; the number of transients (2–16 scans) and the sweep widths were optimized individually. In the homonuclear ^{1}H,^{1}H-COSY (Bruker pulse program *cosygpqf*) and NOESY (*noesygpph*) experiments, the relaxation delay was set to 1.5 s, and the 90° pulse length to 7.5 μs. The resulting free induction decays were zero-filled to a 2 k × 1 k data matrix and apodized with a sine function for COSY and a shifted (π/2) sine function for NOESY in both the ω1 and ω2 dimensions prior to Fourier transformation. 2D NOESY experiments were performed with pulsed filtered gradient techniques. The mixing time was 0.3 s. HSQC experiments (*hsqcetgpsp*) were acquired using adiabatic pulses for inversion of ^{13}C and globally optimized alternating phase rectangular pulse sequence for broadband ^{13}C-decoupling, optimized for ^{1}J(CH) = 145 Hz. The 90° ^{13}C pulse length was 7.5 μs. ^{1}H,^{13}C long-range spectra HMBC (*hmbcgplpndqf*) were performed with ^{n}J(CH) set to 8 Hz.

The dynamic ^{1}H NMR spectra were recorded at different temperatures in the range of 183–323 K in steps of 15 K. Temperature control was achieved using a Bruker variable temperature unit (BVT 3000) in combination with a Bruker cooling unit (BCU-05). The sample was cooled by a flow of low-temperature nitrogen gas from a Dewar with liquid nitrogen. The experiments were performed without sample spinning.

The NMR samples were prepared by additional dissolving in an acetone-d_6 (compound **I**), dichloromethane-d_2 (compound **II**), and chloroform-*d* (compound **III**) solvents. Low-temperature spectra for compounds **II** and **III** were recorded in solvent mixture of $CD_2Cl_2 + (CD_3)_2CO$ (1 : 4) and $CDCl_3 + (CD_3)_2CO$ (1 : 4), respectively. Chemical shifts are given in values of parts per million, referenced to residual solvents signals (acetone-d_6: 2.05 for ^{1}H, 29.92 and 206.68 for ^{13}C; dichloromethane-d_2: 5.32 for ^{1}H, 54.00 for ^{13}C;

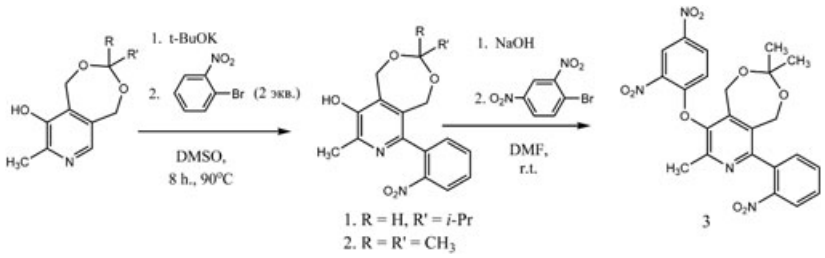

Figure 2. Synthesis scheme of studied compounds.

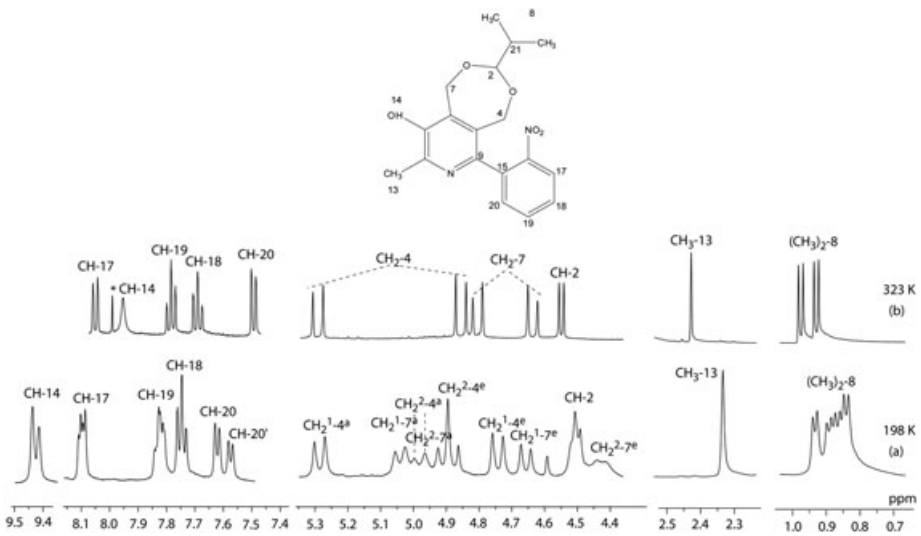

Figure 3. The ^{1}H NMR spectra of compound **I** dissolved in acetone-d_6 at the temperature of 198 K (a) and 323 K (b). Impurity signals are marked by '*'. The signal of CH-21 is not shown because of the overlapping with the solvent signal. Superscripts 1 and 2 correspond to major and minor conformations, respectively; superscripts a and e correspond to pseudo-axial and pseudo-equatorial position relative to the seven-membered ring.

chloroform-*d*: 7.24 for ^{1}H, 77.23 for ^{13}C). All of the samples were prepared in standard 5 mm ampoules. The working concentrations of the substances were 0.5 wt.%, the solution volume was 0.6 mL, and the deuterium signals of the solvents were used for the stabilization of magnetic field.

For the full lineshape analysis, the WinDNMR-Pro 7.1.14 program designed by Hans J. Reich at the University of Wisconsin was used.[16] Activation parameters were calculated using the Eyring equation. The errors in the determination of the $\Delta G^{\neq}$ activation parameters were less than 1 kJ/mol.[17,18]

Free energy of activation of first-order monomolecular reversible reactions, which include intramolecular rotation processes and interconversions of cyclic systems, can be found using the following equations[19–21]:

$$A \underset{k_{ab}}{\overset{k_{ab}}{\rightleftarrows}} B$$

$$\Delta G^{\neq} = \Delta H^{\neq} - T\Delta S^{\neq}$$

$$\ln(k/T) = -\Delta H^{\neq}/RT + \Delta S^{\neq}/R + 23.76$$

where $\Delta H^{\neq}$ is the activation enthalpy, $\Delta S^{\neq}$ is the activation entropy, T is the temperature in K, and R is the universal gas constant.

The semi-empirical calculations were carried out using the HyperChem 8 software. The PM3 computations were performed *in vacuo* with full geometry optimization at each point. For the conformers, we calculated the matrix of second derivatives. All the considered structures had positive frequencies.

Results and Discussion

Dynamic NMR study of compound I

For the chemical structure of compound **I** to be confirmed, 1D ^{1}H, ^{13}C, and 2D NMR experiments were performed. The signals in the ^{1}H NMR spectrum (Fig. 3) were assigned using literature data,[18] 2D ^{1}H-^{1}H COSY (Fig. 4), 2D ^{1}H-^{13}C HSQC, 2D ^{1}H-^{13}C HMBC, and 2D NOESY NMR spectra at the room temperature and at 203 K. The ^{1}H NMR chemical shifts and scalar couplings are presented in Table 1. $CH_2^{1,2}$-4,7^{a,e} signals were assigned according to the literature data.[18]

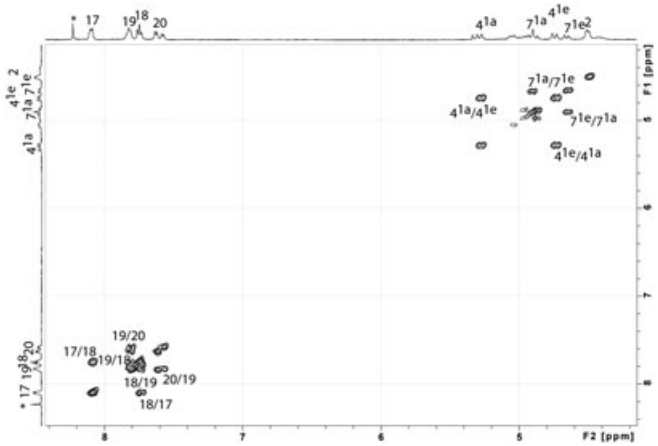

Figure 4. Fragment of ^{1}H-^{1}H COSY NMR spectrum of compound **I** in acetone-d_6 at T = 198 K. Superscripts 1 and 2 correspond to major and minor conformations, respectively; superscripts a and e correspond to pseudo-axial and pseudo-equatorial position relative to the seven-membered ring protons.

Table 1. ^{1}H NMR spectral parameters (δ, ppm) and scalar couplings (J, Hz, in parentheses) of compounds **I**, **II**, and **III** in acetone-d_6 at different temperatures

	T, K		CH–20	CH–19	CH–18	CH–17	CH–21	OH–14	CH–2	CH_3–13	$(CH_3)_2$–8	CH_2–4	CH_2–7
Compound **I**	323		7.49 d (7.5)	7.78 t (7.5)	7.68 t (7.8)	8.04 d (7.8)	1.96 m (6.8)	7.95 b	4.55 (7.1)	2.43	0.95 m (25; 6.8)	5.08 q (15.3)	4.72 q (14.8)
	198	Conf.1	7.62 d (7.5)	7.83 b	7.75 t (7.8; 1.2)	8.09b (7.8)	1.98b	9.44	4.51b	2.33b	0.87 m (25; 6.8)	5.01 q (15.3)	4.80 q (14.8)
		Conf.2	7.57 d (7.5)			8.10 b (7.8)	1.94b	9.41			0.90 m (25; 6.8)	4.93 q (15.3)	4.73 q (14.8)
Compound **II**	183	Conf.1	7.59 b (7.6)	7.74 t (7.8)	7.67 t (7.8)	8.01 d (8.1)	—	9.37 b	—	2.b	1.42 d	4.77 q (15.3)	4.93 q (14.5)
		Conf.2	7.52 b (7.6)	7.84 t (7.8)		8.13 d (8.1)		9.39 b		2.38b	1.33	4.51 q (15.3)	4.93 q (14.5)
Compound **III**	183	Conf.1	7.67 d (7.8)	7.87 b	7.81 b	8.17, 8.20 d (8.1)	CH–25:9.01 b	CH–23:8.57, 8.68 (9.5; 2.7)	CH–226.94, 7.13 d (9.5)	2.21, 2.28	1.28, 1.40	4.84 q (16.8)	4.95 q (17.8)
		Conf.2	7.65 d (7.8)	7.99 b		8.31, 8.33 d (8.1)	CH–25:9.03 b	CH–23:8.54, 8.74 d (9.5; 2.7)	CH–22:7.06, 7.18 d (9.5)	2.29,2.35	1.32, 1.38	4.60 q (16.8)	4.88 q (17.8)

d, doublet; t, triplet; q, quadruplet; m, multiplet; b, broadened signal.

At room temperature, CH_2-4,7 methylene protons are observed in the form of AB-quadruplets because of the chiral C-2 carbon atom. AB-quadruplet with a stronger nonequivalence of the protons is observed for the CH_2-4 group because it is closer to the 2-nitrophenyl rotor of the molecule. At a low temperature, each of the CH_2-4 and CH_2-7 groups is observed in the ^{1}H NMR spectrum as two AB-quadruplets: CH^1_2-4, CH^2_2-4, CH^1_2-7, CH^2_2-7 in the range of $\delta = 4.40–5.30$ ppm. As the temperature decreases, the CH-20 signals split into two doublets ($J = 7.3$ Hz) with the intensity ratio of 2 : 1. The number of the resonance lines of the methyl protons $(CH_3)_2$-8 in the NMR spectrum at 198 K is also doubled from 4 to 8 comparing with that at 323 K.

This lineshape evolution of the spectrum can be explained by slowing down the rotation of nitrophenyl fragment around C9–C15 bond, resulting in the formation of two pairs of conformational diastereomers. This process was studied by lineshape analysis using the signals of OH-14 and CH-20. The chemical exchange rate constants (k) at each temperature were defined using WinDNMR program. The temperature dependence of the chemical exchange rate constants k for the CH-20 signal is shown in Fig. 5. Obtained activation energy is presented in Table 2. Calculated energy barriers are in a good agreement with literature data. Values for similar processes are usually in the range of 37–63 kJ/mol.[22]

Fragment of 2D NOESY spectrum at 223 K is shown in Fig. 6. Cross-peaks between the signals of CH-20 protons and both pseudo-axial and pseudo-equatorial CH_2-4 protons of major and minor conformations are observed in the spectrum simultaneously. It means that the conformational exchange of the cycle between the *chair* and the *twist* forms is still fast in the NMR timescale. In addition, exchange cross-peaks between CH-20 protons in two conformations are observed. Populations of the most stable conformations transformed into each other by a rotation of the nitrophenyl fragment around the C9–C15 bond are in the ratio of 2 : 1.

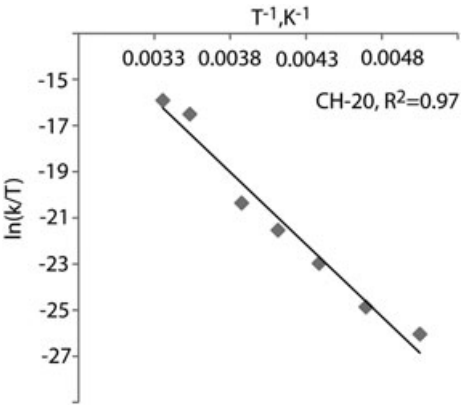

Figure 5. Temperature dependence of the exchange rate constant for the CH-20 signal of compound **I**.

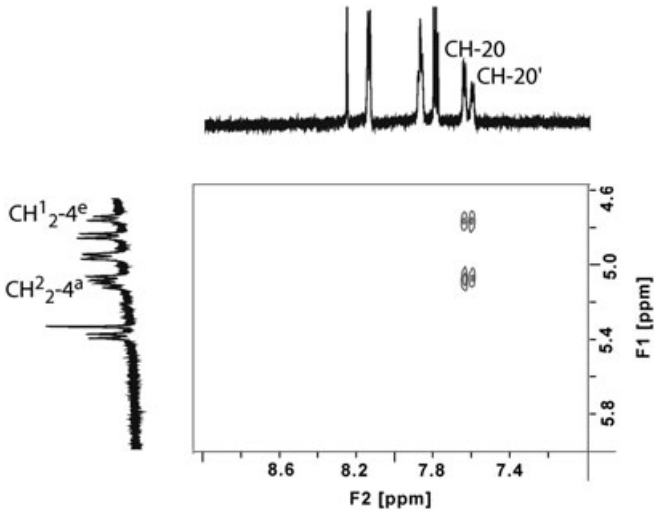

Figure 6. Fragment of the 2D NOESY NMR spectrum of compound **I** at 223 K, $\tau_m = 0.3$ s. Superscripts 1 and 2 correspond to major and minor conformations, respectively; superscripts a and e correspond to pseudo-axial and pseudo-equatorial position relative to the seven-membered ring protons.

Table 2. Activation parameters ($\Delta G^{\neq}_{203K}$, kJ/mol) of the conformational exchange for compounds **I**, **II**, **III**

I (R, C-T)		**II** (R, T-T)		**III** (R′, R, T-T)	
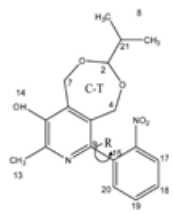		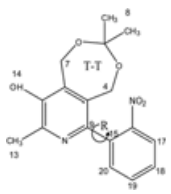		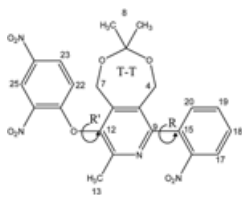	
Experimental free energy barriers, kJ/mol					
R	R	T-T	R′	R	T-T
OH-14:41.4	CH_2-4:9.6	CH_2-4:45.7	$(CH_3)_2$-8:46.0	$(CH_3)_2$-8:40.6	$(CH_3)_2$-8:40.5
CH-20:40.2	CH_3-13:40.7		CH-22:46.0	CH-22:40.4	CH-22:40.5
	CH-20:39.6				
Calculated energy barriers					
41.4	41.4	—	46.9	44.0	—

R, rotation of the nitrophenyl fragment around the C9–C15 bond; R′, rotation of the dinitrophenyl fragment around the C12–O bond; T-T, twist-twist interconversion of the seven-membered ring; C-T, chair-twist interconversion of the seven-membered ring.

Figure 7. The ^{1}H NMR spectra of compound **II** at the temperature of 183 K (a), 198 K (b), and 308 K (c) (in $CD_2Cl_2 + (CD_3)_2CO$). The signals of impurities are marked by asterisks '*'. Superscripts 1 and 2 correspond to major and minor conformations, respectively; superscripts a and e correspond to pseudo-axial and pseudo-equatorial position relative to the seven-membered ring protons.

Dynamic NMR study of compound II

Assignment of the signals in the ^{1}H NMR spectrum (Fig. 7) was performed similarly to compound **I**. The ^{1}H NMR chemical shifts are presented in Table 1.

With temperature decreasing, the signals of CH_2-4 and CH_2-7 groups are broadened and then split into two AB-quadruplets because of the formation of conformational enantiomers. At the same time, the signal of the geminal methyl groups ($(CH_3)_2$-8) remains singlet. At 183 K, the number of lines corresponding to the signals of the aromatic protons CH-17, CH-19, CH-20, the methyl protons CH_3-13, is doubled compared with the spectrum at the room temperature with the ratio intensity of 10 : 1. The number of the lines corresponding to $(CH_3)_2$-8 increased from one to four singlets. The lineshape of the signals of the CH_2-4 and CH_2-7 methylene protons also depends on the temperature. Each of the CH_2-4,7 methylene groups signals (singlets at 308 K) is observed in the form of two AB-quadruplets at a low temperature, but some of the lines are invisible because of overlapping. Lines of the signal CH_2-4 show a larger nonequivalence degree compared with the lines of CH_2-7 because of the influence of closely located nitrophenyl substituent. Such lineshape evolution of the spectrum can be explained by two conformational exchange processes becoming slow in the NMR timescale with the temperature decreasing. Thus, the observed set of signals in the ^{1}H NMR spectrum at 183 K corresponds not only to slowed down rotation of nitrophenyl fragment around C9–C15 bond but also to 'frozen' *twist-twist* interconversion of the cycle.

Lineshape analysis of the NMR signals of CH_3-13, CH-20 protons was performed similarly to compound **I**. Activation energy $\Delta G^{\neq}$ of rotation process (R) is presented in Table 2. The thermodynamic parameters of the rotation and *twist-twist* transformation processes were calculated by the line shape analysis of CH_2-4 protons signals (Fig. 8).

Taking into account the nonlinear temperature dependence of the exchange rate constant for the CH_2-4 signal (Fig. 8), an approach based on the decomposition of lines corresponding to

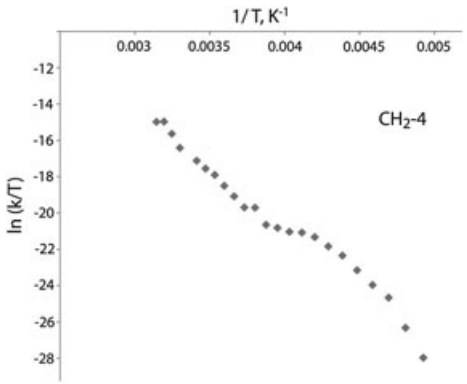

Figure 8. Temperature dependence of the exchange rate constant of the CH_2-4 signal for compound **II**.

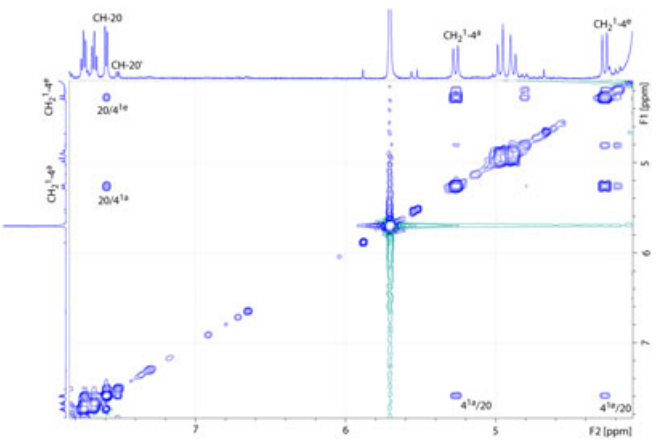

Figure 9. Fragment of the 2D NOESY NMR spectrum of compound **II** at 183 K, $\tau_m = 0.3$ s.

two processes in the program Origin 7.5 was used for the calculation.[11] The results are presented in Table 2.

The fragment of 2D NOESY spectrum at 183 K is shown in Fig. 9. The cross-peaks between the signals of CH-20 protons and both pseudo-axial and pseudo-equatorial protons of CH_2^1-4 corresponding to major conformation are observed in the spectrum. Similar cross-peaks between CH-20′ protons and CH_2^2-4 corresponding to the minor conformation also exist but are invisible in the figure because of a very low intensity. It means that the seven-membered cycle of compound **II** exists in the equilibrium of two *twist* forms compound **I**, which is in a fast exchange between the *chair* and the *twist* forms. Moreover, the rotation of nitrophenyl fragment around C9–C15 bond observed for compound **II** leads to different populations of the most stable major and minor conformations (10 : 1) from those for compound **I** (2 : 1).

Dynamic NMR study of compound III

Assignment of the signals of compound **III** in the ^{1}H NMR spectrum (Fig. 10; Table 1) was made similarly to compounds **I** and **II** and on the basis of 2D ^{1}H-^{1}H COSY spectra.

The signals of CH_2-4 and CH_2-7 groups of compound **III** split into two AB-quadruplets already at 283 K. And in contrast to compound **II**, the geminal methyl groups ((CH_3)$_2$-8) become nonequivalent at the same temperature and their signals split into two singlets. This is the evidence of the fact that the first conformational process becomes slow in the NMR timescale.

At the temperature of 183 K, the number of the resonance lines corresponding to CH-23, CH-22, CH_3-13, and (CH_3)$_2$-8 increased four times compared with the spectrum at the room temperature because of slowing down of the three conformational processes that led to the formation of four pair of conformational diastereomers. Intensities of the lines were in the ratio of 10 : 5 : 1.5 : 1. Moreover, each of CH_2-4,7 methylene protons was observed in the form of two AB-quadruplets at a low temperature (CH_2^1-4, CH_2^2-4, CH_2^1-7, CH_2^2-7) just like it was in the case of compound **II** because of the symmetry. It means that compound **III** also exhibited *twist-twist* (T-T) interconversion of the seven-membered ring that was slowed down at the low temperature.

For assignment of the signals in the ^{1}H NMR spectrum at 183 K, 2D NOESY experiment was carried out. The region of the 2D NOESY spectrum corresponding to the methylene groups (δ = 4.2–5.4 ppm) is shown in Fig. 11. In a range of 183–213 K, four AB-quadruplets with NOE correlations were observed for the methylene protons: CH_2^1-4, CH_2^2-4, CH_2^1-7, CH_2^2-7.

Thus, compound **III** takes part in three intramolecular conformational exchange processes in solution: rotation of the nitrophenyl fragment around C9–C15 bond (R), rotation of dinitrophenyl fragment around C12–O bond (*R*′), and *twist-twist* (T-T) interconversion of seven-membered ring. Activation parameters in compound **III** were also calculated using line shape analysis by WinDNMR program. The peaks of (CH_3)$_2$-8 and CH-22 were chosen as the basic signals for determining the energy parameters. The results are

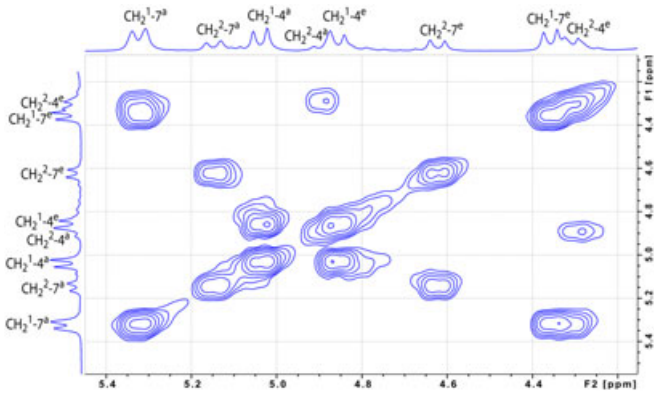

Figure 11. Methylene region of the 2D NOESY NMR spectrum of compound **III** at 183 K, τ_m = 0.3 s. Superscripts 1 and 2 correspond to major and minor conformations, respectively; superscripts a and e correspond to pseudo-axial and pseudo-equatorial position relative to the seven-membered ring protons.

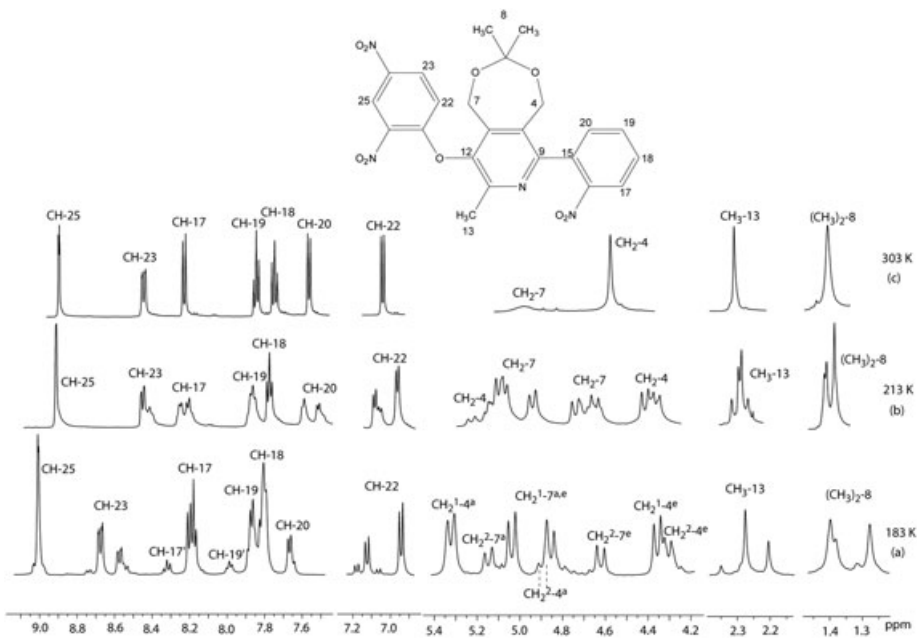

Figure 10. The ^{1}H NMR spectra of compound **III** at the temperature of 183 K (a), 213 K (b), and 303 K (c) ($CDCl_3$ + (CD_3)$_2$CO).

presented in Table 2. Obtained energy barriers are in good agreement with literature data and the values of previously studied pyridoxine derivatives.[11,10]

Semi-empirical calculations

PM3 calculations of rotational barriers using the HyperChem 8 software were carried out in order to relate experimental activation barriers with the conformational processes. During the calculations of the rotation of 2-nitrophenyl moiety, values of the torsion angle $\varphi 1$ (Fig. 12) were changed in steps of 10° and full geometry optimization was carried out at each point. The activation energy was specified by the recalculation with changing of the torsion angle $\varphi 1$ in steps of 2° in the region close to the transition state. The results appeared to be fairly similar for all studied compounds. The 2-nitrophenyl group has twisted conformations with the torsion angles around −70° and 70°. The transition state is shifted by ±8° from the coplanar conformation depending on the conformation of the dioxepine cycle (Fig. 13).

The activation barrier for the R′ process for compound **III** was calculated as described in our previous paper by independent rotating of torsion angles $\varphi 2$ and $\varphi 3$.[11] The resulting potential energy surface is shown in Fig. 14. The geometry of the transition states and the stable conformers were found to be very similar for compound **III** and the previously studied pyridoxine derivatives with 2,4-dinitrophenil moiety at the same position. The optimal conformation of the phenyl group is almost perpendicular ($\varphi 2$ around ±95°, $\varphi 3$ around −170°) to the pyridine ring with 2-nitro group turned away from the system (Fig. 15). However, introducing the 2-nitrophenyl moiety in the *para* position to the 2,4-dinitrophenil fragment increases the calculated activation barrier by 1 kcal/mol. The calculated activation parameters of the conformational exchange are presented in Table 2.

A comparison of the semi-empirical and the experimental data confirms that the R-process in compound **II** has a smaller activation barrier than twist-twist transformation, while the addition of the second rotor group in compound **III** surprisingly results in decreasing of the twist-twist exchange barrier, and the first 'frozen' process, in this case, is the rotation of the 2,4-dintrophenyl moiety.

The comparison of obtained results with our previous studies reveals the significant influence of dynamics of the adjacent conformational processes on each other. It was found that an increase in the seven-membered cycle transformation rate leads to the raise of activation energies for the 2,4-dinitrophenyl group rotation (50–53 kJ/mol for acetal derivatives,[10] 46 kJ/mol for compound **III**, and 41–44 kJ/mol for ketals[11]). The rotation of 2-nitrophenyl group around one single bond is less dependent on the changes of distant substituents, and its activation barriers remain almost the same for all studied compounds. The 2,4-dinitrophenyl group rotating around two single bonds has a greater impact on the

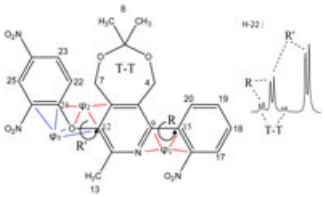

Figure 12. Schematic presentation of the conformational exchange processes for compound **III**: R, R′ show rotations; T-T stands for twist-twist interconversion of the cycle (left) and the line shape of the CH-22 signal at 183 K (right).

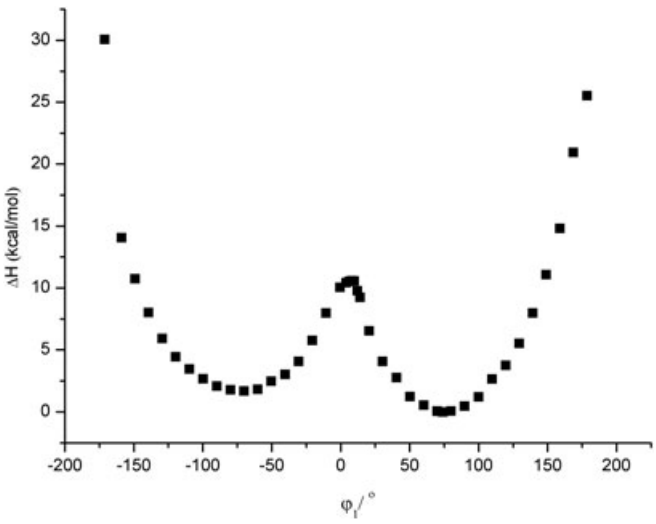

Figure 13. The activation barrier for the R-process of compound **III**.

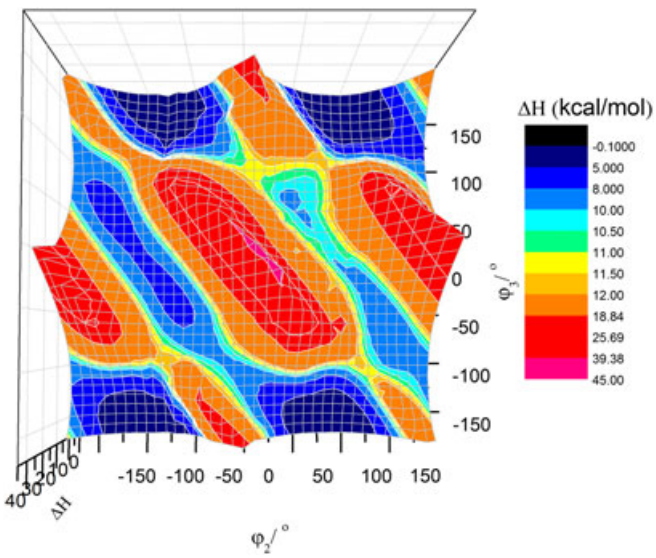

Figure 14. Potential energy surface of the rotation of 2,4-dinitrophenyl fragment around C12-O and O-C21 bonds for compound **III**.

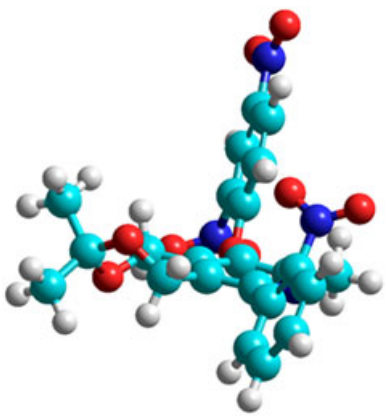

Figure 15. The geometry of the major conformer of compound **III** according to the PM3 calculations.

transformations of the ketal cycle than 2-nitrophenyl rotor at the 6-position of pyridine ring (twist-twist activation barriers are 51 and 46 kJ/mol, respectively[11]). But simultaneous rotation of both groups surprisingly results in significantly lower barriers (40.5 kJ/mol) of twist-twist interconversion in comparison with their separate action.

Conclusions

Conformational features and dynamics for three new pyridoxine derivatives were studied by dynamic NMR and 2D NOESY experiments. It was shown that compound **I** is involved in two conformational exchange processes. The first process is a rotation of 2-nitrophenyl fragment around C9–C15 bond, which was seemed slowed down in DNMR experiments. The second process is *chair-twist* interconversion of the seven-membered cycle, which remained fast relative to the NMR chemical shifts timescale even at the low temperatures. Compound **II** takes part in two conformational exchange processes: *twist-twist* interconversion of the seven-membered cycle and rotation around C9–C15 bond. Three conformational exchange processes are observed for compound **III**: *twist-twist* interconversion of the seven-membered cycle, rotation of the nitrophenyl fragment around C9–C15 bond, and rotation of dinitrophenyl fragment around C12–O bond. Rotations around C9–C15 and C12–O bonds and *twist-twist* interconversion of the seven-membered cycle are well observed in ^{1}H NMR spectra at low temperature. Therefore, activation parameters $\Delta G^{\neq}_{203K}$ for all three processes were calculated using lineshape analysis of DNMR spectra. It was established that the energy barrier of rotation around C12–O bond is about 6 kJ/mol higher than the energy barrier of rotation around C9–C15 bond. Energy barriers of rotation around C9–C15 bond and *twist-twist* interconversion of the cycle for compound **III** have approximately the same values.

Acknowledgements

This work was funded by the subsidy allocated to Kazan Federal University for the project part of the state assignment in the sphere of scientific activities. The work was also performed according to the Russian Government Program of Competitive Growth of Kazan Federal University and supported by Russian Foundation for Basic Research (grant 16-33-60014).

References

[1] I. A. Khodov, S. V. Efimov, V. V. Klochkov, G. A. Alper, L. A. E. Batista De Carvalho. *Eur J Pharm Sci* **2014**, *65*, 65–73.
[2] I. A. Khodov, M. G. Kiselev, S. V. Efimov, V. V. Klochkov. *J Magn Reson* **2016**, *266*, 68–67.
[3] S. V. Efimov, I. A. Khodov, E. L. Ratkova, M. G. Kiselev, S. Berger, V. V. Klochkov. *J Mol Struct* **2016**, *1104*, 63–69.
[4] S. V. Efimov, Y. O. Zgadzay, V. V. Klochkov. *Appl Magn Reson* **2014**, *45* (11), 1225–1235.
[5] A. U. Ziganshin, O. S. Kalinina, A. D. Strelnik, M. R. Garipov, S. A. Koshkin, L. E. Ziganshina, Y. G. Shtyrlin. *Int J Pharm* **2015**, *11*(4), 400–404.
[6] M. V. Pugachev, N. V. Shtyrlin, L. P. Sysoeva, E. V. Nikitina, T. I. Abdullin, A. G. Iksanova, A. A. Ilaeva, R. Z. Musin, E. A. Berdnikov, Y. G. Shtyrlin. *Bioorg Med Chem* **2013**, *21*(14), 4388–4395.
[7] A.R. Kayumov, A.A. Nureeva, E.Y. Trizna, G.R. Gazizova, M.I. Bogachev, N. V. Shtyrlin, M.V. Pugachev, S.V. Sapozhnikov, Y.G. Shtyrlin, Bio Med Research International, **2015**, Article ID 890968, 10 pages, doi:10.1155/2015/890968.
[8] N. V. Shtyrlin, O. A. Lodochnikova, Y. G. Shtyrlin. *Mendeleev Commun* **2012**, *22*(3), 169–170.
[9] A. D. Strelnik, A. S. Petukhov, I. V. Zueva, V. V. Zobov, K. A. Petrov, E. E. Nikolsky, K. V. Balakin, S. O. Bachurin, Y. G. Shtyrlin. *Bioorg Med Chem Lett* **2016**, *26*(16), 4092–4094.
[10] I. Z. Rakhmatullin, L. F. Galiullina, M. R. Garipov, A. D. Strel'nik, Y. G. Shtyrlin, V. V. Klochkov. *Magn Reson Chem* **2014**, *52*(12), 769–778.
[11] I. Z. Rakhmatullin, L. F. Galiullina, M. R. Garipov, A. D. Strel'nik, Y. G. Shtyrlin, V. V. Klochkov. *Magn Reson Chem* **2015**, *53*(10), 805–812.
[12] A. S. Petukhov, A. D. Strel'nik, V. Y. Fedorenko, I. A. Litvinov, O. A. Lodochnikova, Y. G. Shtyrlin, E. N. Klimovitskii. *Zh Obsh Khim* **2007**, *77*(8), 1339–1344.
[13] Y.G. Shtyrlin, V.Y. Fedorenko, E.N. Klimovitskii, *Zh Obshch Khim*, **2001**, *71*, 5, 872.
[14] A. D. Strel'nik, M. R. Garipov, A. S. Petukhov, N. V. Shtyrlin, O. A. Lodochnikova, I. A. Litvinov, A. K. Naumov, O. A. Morozov, A. E. Klimovitskii, Y. G. Shtyrlin. *Spectrochim. Acta Mol Biomol Spectrosc* **2014**, *117*, 793–797.
[15] Y.G. Shtyrlin et al, Pat. RU2501801, MPC C07D491/056, 20.12. **2003**.
[16] H.J. Reich, University of Wisconsin, WINDNMR-Pro, a windows program for simulating high-resolution NMR spectra. http://www.chem.wisc.edu/areas/reich/plt/windnmr.htm **2002** [11February 2002]
[17] N. M. Sergeev. *Uspehi Khimii* **1973**, *42*(5), 789–798.
[18] F. H. Karataeva, V. V. Klochkov, *^{1}H and ^{13}C NMR Spectroscopy in Organic Chemistry*, Kazan state university, Kazan, **2007**.
[19] S. Benson, *Fundamentals of Chemical Kinetics*, Mir, Moscow, **1964**.
[20] N. M. Emanuel, D. G. Knorre, *Course of Chemical Kinetics*, Vyshaya shcola, Moscow, **1984**.
[21] S. G. Entelis, R. P. Tiger, *The Kinetics of Reactions in the Liquid Phase*, Quantitative account of the influence of the environment, Khimiya, Moscow, **1973**.
[22] L. M. Jackman, F. A. Cotton, *Dynamic Nuclear Magnetic Resonance Spectroscopy*, Academic Press, N.Y., San Francisco, London, **1975**.